

X-ray radial distribution analysis of amorphous $\text{Bi}_2\text{O}_3\text{-B}_2\text{O}_3\text{-TeO}_2$ (BBT)

A. ABOU SHAMA*, A. ABD-ALLAH, G. MA. YOUSSEF

Physics Department, Faculty of Science, Ain Shams University, 11566 Abbassia, Cairo, Egypt

Short range order (SRO) and Medium range order (MRO) of the amorphous $[\text{xBi}_2\text{O}_3\text{-(0.5-x)B}_2\text{O}_3](0.5\text{TeO}_2)$ with $\text{x}=0.05, 0.1, 0.2,$ and 0.3 respectively were studied with the application of X-ray radial distribution analysis. This set of samples was prepared by the melt rapid quenching technique of its initial reagents. The extracted information for the first ordered shells in the real space clearly showed the role of increased percents of Bi_2O_3 . The role of Bi_2O_3 introduced in the matrix was found to increase the amorphous network order besides its ability to modify the atomic correlated distances of the detected atomic pairs and also their coordination numbers. The first ordered shell in SRO was belonging to Te-O pairs arranged in the form TeO_4 at nearly 1.96\AA with an evolution of Te-O pairs with Non-Bridging Oxygen (NBO) at nearly 1.83\AA . The correlated Bi pairs of oxygen environment were revealed at 2.57\AA for $\text{x}=0.05, 0.1, 0.2$ and this distance was highly stretched at $\text{x}=0.3$ to be 2.75\AA with a distorted pyramidal form. The Te-Te and Bi-Bi atomic pairs were observed at $3.85\text{\AA}, 4.35\text{\AA}$ for $\text{x}=0.05$ and 0.2 . The previous pairs had contracted distances, $3.75\text{\AA}, 4.20\text{\AA}$ for $\text{x}=0.1$ and 0.2 respectively. The B-O and/or B-B correlations were not evidenced due to the weak scattering strength of B_2O_3 to X-ray compared to other heavier components. The previous atomic pairs of Te-Te and Bi-Bi had a layered structure in the MRO region. The bond angle distributions of different atomic pairs were also reported as a function of x and thrown an increased structural information on the studied amorphous system.

(Received January 25, 2013; accepted May 15, 2014)

Keywords: Non-Bridging Oxygen (NBO), Bridging oxygen (BO), Distorted octahedral glasses and pyramidal units

1. Introduction

It is widely known that glasses containing heavy metal oxides show various attractive optical features such as high refractive index, high third order optical nonlinearity and high transmittance in near-IR [1]. Recently, multi oxide component glasses, $\text{La}_2\text{O}_3, \text{Nb}_2\text{O}_5, \text{WO}_3, \text{PbO}, \text{TeO}_2$ and Bi_2O_3 have been commercially developed and manufactured to achieve the high refractive index to be as high as ~ 2 . Generally, high refractive index glasses show coloring which is mainly caused by the optical absorption edge which locates not in deep-UV but in near visible wavelength [1].

The optical nonlinearity of high refractive index glasses have been studied in various types of glasses so far, such as Pb, Bi, Te containing glasses and chalcogenide glasses [2-4]. The previous glasses had excellently high third order nonlinear susceptibility up to $\chi^3 \sim 10^{-11}$ esu. In recent years also, the bismuth based glasses such as $\text{Bi}_2\text{O}_3\text{-B}_2\text{O}_3\text{-WO}_3$ have attracted great attentions due to their abilities to be used in all optical switching, wavelength conversion and high speed time division multiplexing, which can improve the communication network of national defences [5].

Tellurite glasses have drawn much attention recently and are considered as promising materials for a variety of optical devices such as optical switches, fibers and optical storage devices due to their high transmittance from the visible to mid-infrared(MIR) spectral regions, also high

refractive index($n > 2$) and unique non-linear optical properties as in Bismuth based glasses[6].

The corresponding amorphous phases by many authors [1,6] are only characterized by XRD to confirm the formation of the amorphous matrix without going in more structural details. The XRD patterns showed the glass ceramics formed in the system $75\text{TeO}_2\text{-}13\text{Bi}_2\text{O}_3\text{-}12\text{ZnO}$, other more very recent compositions of the same ternary given system are formed. All the previous glass samples were heated at 330°C for 64h giving up $\text{Bi}_{0.864}\text{Te}_{0.136}\text{O}_{1.568}$ of a completely crystallized phase of an orthorhombic structure with PDF#38-0865.

The Raman spectra of the $\text{Bi}_2\text{O}_3\text{-TeO}_2\text{-ZnO}$ and the optical micrographs confirmed their high transparency in the near and mid infrared (MIR) regions. Also, as the Bi_2O_3 content increased in the glass composition, the obtained crystallization tendency is enhanced and high crystal concentrations were obtained[6]. Murugan et al.[7-9] reported that the phase $(1-x)\text{Li}_2\text{B}_4\text{O}_7\text{-xBi}_2\text{WO}_6$ (with $0.0 \leq x \leq 0.35$) was an amorphous as quenched glass and it was treated at $720\text{K}(T_{\text{cri}})$ for 6h to be changed into orthorhombic phase of Bi_2WO_6 (BW). This orthorhombic phase of BW had $a=4.5496\text{\AA}, b=5.4511\text{\AA}$ and $c=16.6462\text{\AA}$ established the crystallization and growth of BW phase in the previous treatment process. Also, Charton et al.[10] recently prepared transparent $(1-x)\text{TeO}_2\text{-xWO}_3$ glasses ($0.0 \leq x \leq 0.325$ mol) by the fast quenching technique and they applied several complementary techniques as IR, XPS and X-ray absorption spectroscopy to approach the structure of these

tungsten oxide-tellurite glasses. Their observed structural results of these investigated glasses showed that the presence of characteristic tellurium environment which vary with the chemical composition of the prepared glassy matrix to be in the trigonal bipyramid TeO_4E units ($x=0$) and changed to trigonal pyramids TeO_3E for high WO_3 content. The tungsten ions always adopt an octahedral configuration.

The objective of this study is mainly focusing on the application of the radial distribution analysis of the collected XRD data of the given amorphous samples to extract the structural information in the SRO and MRO regions (due to rarely published articles concerning this task). Also, a reported bond angle distributions of different detected atomic pairs are given in relation to the introduced percents of Bi_2O_3 .

2. Experimental

2.1. Preparation of the glass specimens

Glass batches were prepared from chemically pure raw materials. The orthoboric acid (H_3BO_3) was used to obtain boron oxide B_2O_3 . Bismuth oxide was introduced in the form of powder of Bi_2O_3 with purity 99.99%. Tellurium oxide (TeO_2) was introduced as such with the ratio 0.5 equals the other ratio of bismuth borate oxides.

The chemicals used were accurately weighed by using an electronic balance. The chemicals were then thoroughly mixed and porcelain crucibles containing the batch were placed in electrically heated furnaces and kept at 950°C for two hours under normal atmospheric conditions. The crucibles were removed from the furnaces and rotated through to produce homogeneous glass.

The glass was cast at a preheated stainless steel molds with radius 1.3cm. All the glasses were properly annealed at 400°C temperature in a muffle furnace, then, the muffle furnace was left to cool at a rate of $30^\circ\text{C}/\text{hour}$ down to room temperature. Annealing process was done to avoid and minimize the stresses and strains, which may be found in the final glass product. The samples were grounded and highly polished before measurements.

The densities of the prepared glass samples were measured in an indirect method based on Archimedes' principle using xylene as an immersion liquid according to the equation:

$$\rho = \text{wt}_a / [\text{wt}_a - \text{wt}_{\text{liq}}] \times \rho_{\text{liq}} \quad \text{gm/cm}^3$$

Where:

- 1) ρ is the required glass sample density
- 2) wt_a is the weight of the glass sample in air
- 3) wt_{liq} is the weight of the glass sample in the immersing liquid
- 4) ρ_{liq} is the density of the immersing liquid

The composition and the density of the glass samples used in this study are shown in the following table [Table 1]:

Table 1. Composition and density of the studied glass batches.

x percent	$\text{Bi}_2\text{O}_3\%$	$\text{B}_2\text{O}_3\%$	$\text{TeO}_2\%$	Bi%	Te%	B%	O%	$\rho_{\text{gm/cm}^3}$
0.05	0.173	0.234	0.593	0.155	0.474	0.074	0.297	4.679
0.1	0.302	0.181	0.517	0.271	0.413	0.057	0.259	3.700
0.2	0.488	0.108	0.421	0.431	0.329	0.034	0.206	5.050
0.3	0.598	0.0599	0.350	0.537	0.273	0.019	0.171	5.407

2.2. XRD apparatus setup

The present data were collected by using Philips (X'pert MPD) diffractometer using the Bragg-Brentano para-focusing technique. Highly monochromated Cu-radiation (wavelength $\lambda=1.541\text{\AA}$) was used. The step scan mode was applied in the 2θ -range ($4-157.4612^\circ$). The step size ($\Delta 2\theta=0.04$) and the counting time was 10 seconds for each reading. The corresponding accessible maximum scattering vector magnitude, K , was 8.0\AA^{-1} ($K=4\pi \sin\theta / \lambda$). The air scattering was avoided by a suitable applied arrangement of XRD system. The receiving and divergence slits were properly chosen in both small and large 2θ -ranges, in order to improve the qualities of data collected as it could as it possible.

2.3. The relation between S (K) and RDF (r)

The scattered intensity in the K-space, $I(K)$, was corrected for the polarization and absorption, scaled and

normalized to get on the self scattered intensity and the structure factor $S(K)$ in the reciprocal space [11-13]. The total structure factor of a glass is given as [11]:

$$S(K) = \{ I(K) - [\langle f^2 \rangle - \langle f \rangle^2] \} / \langle f \rangle^2 \quad (1)$$

Where the term $[\langle f^2 \rangle - \langle f \rangle^2]$ is known as the Laue diffraction and is more significant at small angle 2θ of X-ray scattering. The RDF is given as:

$$\text{RDF} = 4\pi r^2 \rho(r) = 2r/\pi \int K[S(K)-1] \exp(-\alpha^2 K^2) \sin(Kr) dK \quad (2)$$

ρ is the sample density in gm/cm^3 , $\rho(r)$ is being the sample atomic density as a function of the radial distance r , α is the disordering parameter of value $\sim 0.1\text{\AA}$ which is mainly used to reduce the effect of spurious details in the high K -range in the measured data.

3. Results

Fig. 1 shows the structure factor $S(K)$ versus K for the given set of samples having 0.05, 0.1, 0.2 and 0.3 percents respectively of Bi_2O_3 . The value of K was in the range $0.3\text{-}8.0 \text{ \AA}^{-1}$ in an observed limitation due to the applied X-ray

radiation of Cu source having $\lambda=1.541 \text{ \AA}$. The Fourier transform was carried out on the $S(K)$ to get on RDF structural information in the real space. The first maxima of both SRO and MRO were revealed showing the first ordered atomic correlations.

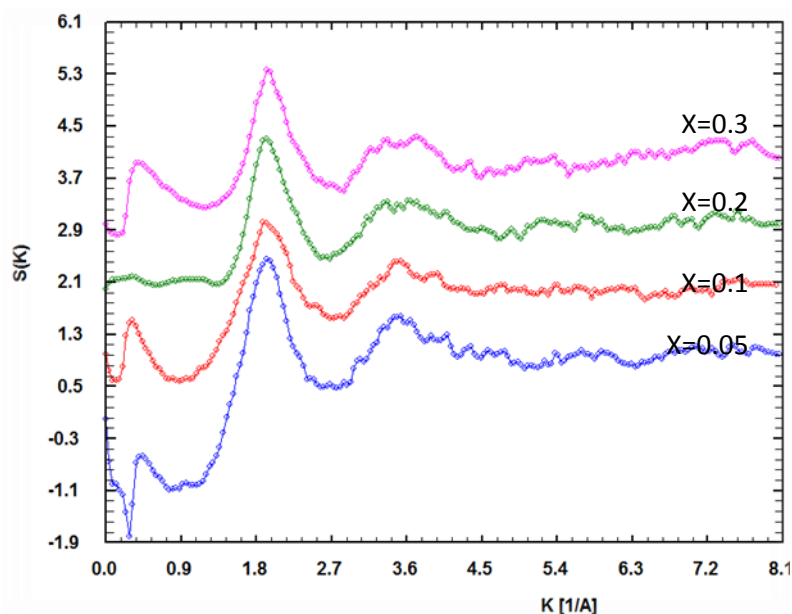


Fig. 1. The structure factor $S(K)$ versus K in the reciprocal space for the amorphous $\text{Bi}_2\text{O}_3\text{-B}_2\text{O}_3\text{-TeO}_2$ with Bi_2O_3 percent, 0.05, 0.1, 0.2, and 0.3 respectively from bottom to top.

Fig. 2 illustrates the variation of the radial distance r , in Å with the obtained RDF (Atoms/ Å^2) for the investigated amorphous system. The first ordered coordination shells were revealed for the studied glasses

and each ordered shell is characterized by three main parameters; its location(peak maximum), its weighted peak area(coordination number) and its full width half maximum(degree of disorder).

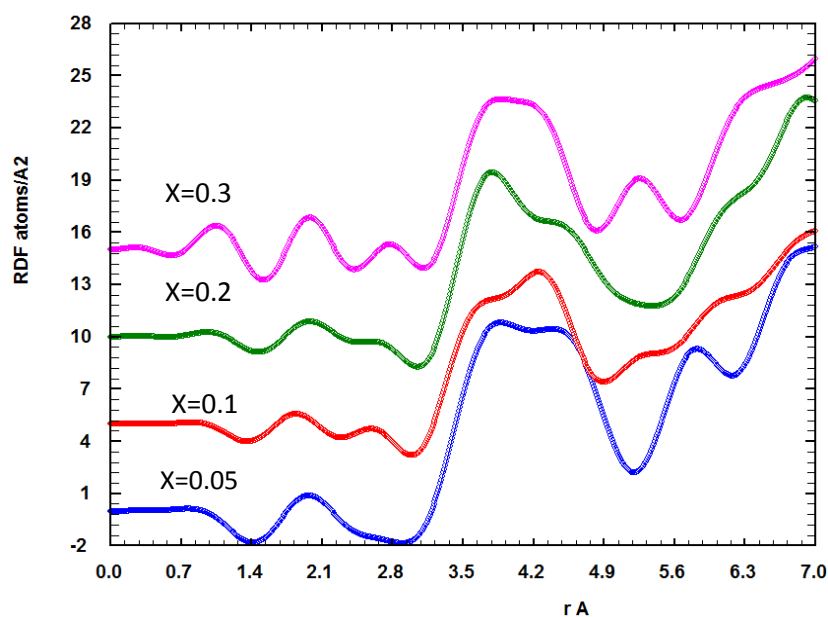


Fig. 2. The RDF against the radial distance r for the amorphous $\text{Bi}_2\text{O}_3\text{-B}_2\text{O}_3\text{-TeO}_2$ with Bi_2O_3 percent, 0.05, 0.1, 0.2 and 0.3 respectively from bottom to top.

4. Discussion

In fig. 1 the first non-Bragg peak was assigned around 2\AA^{-1} and the second broad peak in the K-space was declared around 3.45\AA^{-1} extended to $\sim 4.85\text{\AA}^{-1}$. In the vicinity of an increased K, after 5\AA^{-1} , no, significant structural order except in the case of $x=0.2$ which suffers some degree of ordering beyond 5\AA^{-1} .

As given in Fig. 2, the RDF against r, the first ordered shell was observed at nearly 2.0\AA which belongs to Te-O correlations having a form of tetrahedral arrangement (TeO_4) for all matrix compositions. The formation of Te-O correlations having non-bridging oxygen (NBO) environment was noted in the second sample ($x=0.1$) to be at 1.825\AA . The evolution of Te-O of NBO nature is mainly due to the introduction of Bi_2O_3 in the amorphous matrix which having the role of Bi^{3+} -ions as a modifier component. The next coordination shell was detected at 2.57\AA in the first three samples, while it was highly stretched in the last sample ($x=0.3$) to be at 2.755\AA . This peak indicates to the presence of Bi-O coordinations having a coordination number of about three. The shift of the previous peak to the longer distance reflects the increase of order of MRO due to the increased percent of Bi_2O_3 relatively to the other components as reported in table.1. The second stronger shell is composed of not resolved two maxima at the ranges; ($3.75\text{-}3.85\text{\AA}$), ($4.2\text{-}4.4\text{\AA}$) respectively and a total coordination number in the range (14-21). This second complex shell is referring to Te-Te and Bi-Bi atomic pairs. The pairs of Te-Te were assigned at 3.85\AA for $x=0.05$ and 0.3 and it were shortened to be at 3.758\AA at $x=0.1$ and 0.2 respectively. The previous change in the Te-Te distances may indicate to the possibility of Bi-atoms or ions to substitute Te-atoms in the MRO region which having larger radius compared to

Te atoms and due to also the increased percents of Bi_2O_3 introduced in the studied system. Also, the presence of Bi-atoms or ions can activate the matrix to be highly ordered in the vicinity of MRO region. The arranged pairs of both Te-Te and Bi-Bi in the MRO had a layered structure. The environment of Bi, however it was of oxygen or bismuth, is always of octahedral form while those of Te coordinated by oxygen or tellurium will be in the form of tetrahedral polyhedron. The small percents of Bi_2O_3 will cause the shortening of Te-Te and Bi-Bi correlated distances which means the increased order of the amorphous matrix in the vicinity of SRO region. The next shell extends from $5.79\text{-}6.19\text{\AA}$ with the change of x is evidencing to Te-O of the second order correlations in the extended MRO region of TeO_4 arranged units. One can again observe the increased order of the concerned system in its MRO-range due to the increased percents of Bi_2O_3 which is presented in form of elongated distances of different correlated atomic pairs. The main findings obtained in this study are confirmed by other workers [6,7-9] and supported our RDF structural information. The different linkages of Te-O-Te and/or Te-O-Bi in the SRO region and Bi-O-Bi, Te-O-Bi in the MRO-range are competitive and connective tissues in both SRO and MRO regions [1, 3, 4]. The different bond angles of different atomic correlated pairs in SRO and MRO regions are reported in the following section.

5. Bond angle distributions

The different bond angle distributions of the observed correlated pairs will also throw some of lights of their order-disorder in both SRO and MRO extended ranges. Table 2 will gather these different bond angles to facilitate the comparison in between.

Table 2. Bond angle distributions of different atomic pairs (in degrees).

Sample No.	x percent	Te- \hat{O} -Te	Te- \hat{O} -Bi	Bi- \hat{O} -Bi	Bi- \hat{O} -Te
1	0.05	163.777	82.105	118.493	97.826
2	0.1	180.000	88.766	111.019	94.509
3	0.2	149.496	82.760	117.639	93.727
4	0.3	156.869	88.732	99.648	88.941

As a result from the previous table, the different atomic linkages in the SRO and MRO regions are composition dependent of the studied amorphous system. It can be concluded from the previous table that with the increase of x the linkages of Bi- \hat{O} -Te inside MRO are highly relaxed (88.941°) compared to Bi- \hat{O} -Bi (99.648°). The sample two having $x=0.1$ had the highest distorted Te- \hat{O} -Te (180°) connections, meanwhile, the sample one ($x=0.05$) had the maximum relaxed Te- \hat{O} -Bi (82.105°). As another finding from table 2, the atomic linkages of both Bi- \hat{O} -Bi and Bi- \hat{O} -Te are generally of increased relaxation (decrease of bond angle) with the increase of x.

The change of the bond angle represents a main reason in the change of the measured physical properties of the systems under study. The more relaxed bonds will have less strains and vice versa for the less relaxed ones which will have an increased stresses and increased positive energy.

6. Conclusions

- The arranged atomic Te-O pairs were in the form of TeO_4 while Bi-O pairs were formed in the form of BiO_6 units (inside MRO).

- The introduction of Bi₂O₃ in the amorphous matrix with small percents causes the increased order in the SRO region, while its increased percents activate more ordering in the vicinity of MRO region.

- The atomic pairs of Te-Te and Bi-Bi had a layered structure in the MRO region.

- Both of obtained structural information from RDF in the real space and bond angle distributions of different atomic pairs are composition dependent.

- The increased percents of Bi₂O₃ increase the packing of the samples through its increased densities with the increase also of Bi-ions percent.

- The introduced Bi₂O₃ in the given amorphous matrix will increase the possibility of substituting some of Te atoms by Bi-ones with the increase of x.

- The findings reported in this manuscript can be supported by another physical studies to throw more views about their promising applications taking in the same time this XRD-RDF data as an important key.

References

- [1] T. Hasegawa, J. of Non-Crystalline Solids, **357**, 2857 (2011).
- [2] D. W. Hall, M. A. Newhouse, N. F. Borelli, W. H. Dumbaugh, D. L. Wiedman, Appl. Phys. Lett., **54**, 1293 (1989).
- [3] S.H. Kim, T. Yoko, S. Sakka, J. Amer. Ceram. Soc. **76**, 2485 (1993).
- [4] N. Sugimoto, H. Kanbara, S. Fujiwara, K. Tanaka, Y. Shimzugawa, K. Hirao, Opt. Soc. Amer., **B16**, 1904 (1999).
- [5] C. Z. Chi, Y. B. Liao, S. R. Lai, Laser Journal, **5**, 1 (2001).
- [6] X. Hu, G. Guery, J. Boerstler, J. D. Musgraves, D. Vanderveer, P. Wachtel, K. Richardson, J. of Non-Crystalline Solids **358**, 952 (2012).
- [7] G. Senthil Murugan, K. B. R. Varma, Materials Res. Bull., **34**, 2201 (1999).
- [8] G. Senthil Murugan, K.B.R. Varma, J. of Non-Cryst. Solids, **279**, 1 (2001).
- [9] G. Senthil Murugan, K. B. R. Varma, Solid State Ionics, **139**, 105 (2001).
- [10] P. Charton, L. Gengembre, P. Armand, J. of Solid State Chem., **168**, 175 (2002).
- [11] A. C. Wright, C. A. Yarker, P. A. V. Johnson, R.N. Sinclair, J. of Non-Cryst. Solids, **104**, 323 (1988).
- [12] J. Krogh-Moe, Acta Cryst. **9**, 951 (1956).
- [13] N. Norman, Acta Cryst. **10**, 370 (1957).

*Corresponding author: aliaboshama_1@hotmail.com
aboushamaali@yahoo.com